Stem Cell Reports
Article

ISSCR

OPEN ACCESS

Loss of mismatch repair promotes a direct selective advantage in human stem cells

Kirby Madden-Hennessey,[1] Dipika Gupta,[1,2] Alexander A. Radecki,[1] Caroline Guild,[1] Abhijit Rath,[1] and Christopher D. Heinen[1,*]

[1]Center for Molecular Oncology, UConn Health, Farmington, CT 06030-3101, USA
[2]Present address: Department of Biochemistry and Molecular Pharmacology, New York University School of Medicine, New York, NY 10016, USA
*Correspondence: cheinen@uchc.edu
https://doi.org/10.1016/j.stemcr.2022.10.009

SUMMARY

Lynch syndrome (LS) is the most common hereditary form of colon cancer, resulting from a germline mutation in a DNA mismatch repair (MMR) gene. Loss of MMR in cells establishes a mutator phenotype, which may underlie its link to cancer. Acquired downstream mutations that provide the cell a selective advantage would contribute to tumorigenesis. It is unclear, however, whether loss of MMR has other consequences that would directly result in a selective advantage. We found that knockout of the MMR gene *MSH2* results in an immediate survival advantage in human stem cells grown under standard cell culture conditions. This advantage results, in part, from an MMR-dependent response to oxidative stress. We also found that loss of MMR gives rise to enhanced formation and growth of human colonic organoids. These results suggest that loss of MMR may affect cells in ways beyond just increasing mutation frequency that could influence tumorigenesis.

INTRODUCTION

The mismatch repair (MMR) pathway maintains genomic stability within a cell. In particular, MMR corrects mistakes made by the DNA polymerase during replication (Fishel, 2015; Kolodner, 1996; Modrich, 2006). This highly conserved repair pathway is initiated by a heterodimer of MSH2-MSH6 recognizing the DNA mismatch during replication (Fishel, 2015). Interaction with the mismatch stimulates an ADP→ATP exchange, resulting in formation of a sliding clamp, which diffuses along the DNA (Fishel, 2015). This ATP-bound clamp recruits the next MMR heterodimer, MLH1-PMS2, to load onto DNA (Fishel, 2015). MLH1-PMS2 then interacts with PCNA (proliferating cell nuclear antigen) located at a strand discrimination site, thought to be a nick in the daughter strand, to activate an inherent endonuclease activity in PMS2 (Pluciennik et al., 2010). Generation of these secondary nicks by PMS2 likely promotes removal of the errant daughter strand through excision by EXO1 or some other exonuclease-independent mechanism (Fishel, 2015; Goellner et al., 2015). The DNA polymerase then resynthesizes the region to insert the correct base. Therefore, loss of function of any of the four major MMR proteins leads to uncorrected mismatches and an ~1,000-fold increase in mutation accumulation as well as increased frameshift alterations in simple repeat sequences (Kunkel and Erie, 2005; Strand et al., 1993).

Acquisition of this mutator phenotype is thought to underlie the link between MMR deficiency and tumorigenesis (Fishel and Kolodner, 1995). Germline mutations in any of the four major MMR genes have been linked to the hereditary form of colon cancer, known as Lynch syndrome (LS; MIM: 120435), and loss of MMR function has also been observed in some sporadic cases of colon and several other cancers (Lynch et al., 2015). The presumption is that MMR genes do not act as classic tumor suppressors whose loss leads to an immediate selective advantage but, rather, indirectly affect tumor etiology by establishing a mutator phenotype that increases the frequency of subsequent mutations in oncogenes and tumor suppressor genes (Fishel and Kolodner, 1995).

It is not clear, therefore, whether there is an immediate effect of MMR loss in a cell before accumulation of mutations in other cancer-driving genes (Fishel, 2001; Heinen et al., 2002). A potential effect may stem from other MMR functions. In addition to repairing polymerase errors, MMR also plays a role in inducing cell cycle arrest and apoptosis in response to certain forms of DNA damage (Gupta and Heinen, 2019; Li et al., 2016). Our lab and others have shown that MMR-deficient cells are more resistant to certain DNA-damaging agents, such as S_N1 alkylating agents (Gupta and Heinen, 2019; Heinen, 2014). The MMR pathway induces a damage response to other agents as well (Aebi et al., 1996; Carethers et al., 1999; Fink et al., 1996; Swann et al., 1996), including 6-thioguanine, 5-fluorouracil, the intrastrand crosslinker cisplatin, and oxidative damage, but there are conflicting data concerning this last source of damage (DeWeese et al., 1998; Glaab et al., 2001; Hardman et al., 2001; Martin et al., 2009, 2010; Wang et al., 2005). These observations invoke the possibility that loss of MMR function could result in an immediate selective advantage under certain environmental conditions that would be independent of subsequent mutational events in other genes.

To study the immediate consequences of MMR loss in human cells, we examined human pluripotent stem cells, a non-cancer model that has yet to acquire multiple mutational changes and undergo subsequent rounds of selection. We have demonstrated previously that this model, including human embryonic stem cells (hESCs), shows robust MMR activity and readily undergoes apoptosis in response to a DNA-alkylating agent in an MMR-dependent manner (Gupta et al., 2018; Lin et al., 2014). In this study, we find that knocking out the MMR gene *MSH2* (MIM: 609309) causes hESCs to gain a selective advantage over wild-type (WT) cells in a standard cell culture environment. We also find that oxidative damage likely plays an important role in selecting for MMR-deficient stem cell populations. These results support the idea that loss of MMR causes a survival advantage in a stem cell population and that certain environmental stresses can increase the selection for MMR-deficient cells.

RESULTS

MMR loss confers a growth advantage in human stem cells

While culturing WT and *MSH2* knockout (KO) hESCs generated by Clustered Regularly Interspaced Short Palindromic Repeats (CRISPR) editing, we consistently observed that the *MSH2* KO hESCs displayed an apparent growth advantage under standard cell culture conditions. To quantify this apparent advantage, we counted the number of cells per well for MMR-proficient WT and two independent *MSH2* KO hESC lines (Figures 1A and 1B). We found that both *MSH2* KO lines showed a significant increase in the number of cells over a 5-day period compared with the WT cells. In addition, we found that multiple other independent *MSH2* KO cell lines also displayed this apparent growth advantage (Figures S1A–S1C). To explore whether this phenotype applied to other stem cell lines, we also knocked out *MSH2* in the human induced pluripotent stem cell (iPSC) line YK26 (Figures S1D and S1E). Similar to the *MSH2* KO H1 hESCs, the YK26 *MSH2* KO line had significantly more cells per well compared with the WT YK26 cells, suggesting that this phenotype was not restricted to H1 hESCs (Figure 1C).

One of the known hallmarks of MMR deficiency is an increase in mutation rate, referred to as the mutator phenotype (Fishel and Kolodner, 1995). Therefore, to verify that the growth advantage observed in *MSH2* KO cells is a result of loss of MSH2 function and not due to downstream changes in other genes, we used CRISPR gene editing to correct the *MSH2* sequence at both alleles in the *MSH2* KO2 cells (Figure S1F). We confirmed that this resulted in restoration of a functional MSH2 protein via western blot as well as restored sensitivity to the DNA-alkylating agent *N*-methyl-*N*′-nitro-*N*-nitrosoguanidine (MNNG) in the *MSH2* knockin (KI) line (Figures S1G and S1H). Restoration of MSH2 significantly reduced the growth advantage; KI hESCs grew less than the parental *MSH2* KO2 line (Figure 1D). We also examined whether this growth advantage was specific to *MSH2* loss or loss of MMR function in general, by utilizing cells in which the *MLH1* (MIM: 120436) gene was knocked out by CRISPR gene editing (Rath et al., 2022). We saw a similar growth advantage in *MLH1* KO cells, much like when MSH2 was lost (Figure 1E), suggesting that the advantage was due to loss of MMR function.

Loss of MMR does not affect cell cycle duration

We next assessed whether the *MSH2* KO growth advantage was due to increased proliferation. We determined that there was no significant difference in the doubling time between *MSH2* KO and WT cells by incubating cells with carboxy-fluorescein diacetate succinimidyl ester (CFSE) (Figure S2A). Our observed doubling time of 14–15 h is consistent with that reported previously for hESCs (Becker et al., 2006). Cell cycle analysis showed no significant difference in the percentage of cells in each phase of the cell cycle between the *MSH2* KO and WT lines (Figure S2B). These data indicate that the growth advantage in the *MSH2* KO cells is not a result of increased proliferation.

MMR-proficient stem cells display increased anoikis levels under standard cell culture conditions

We have shown previously that *MSH2* KO hESCs are more resistant to the DNA-damaging agent MNNG compared with MMR-proficient hESCs (Gupta et al., 2018; Rath et al., 2019). This suggests that, in the presence of an exogenous DNA-damaging agent, MMR-deficient cells have a survival advantage over MMR-proficient cells. Therefore, we hypothesized that the growth advantage displayed by *MSH2* KO hESCs could be due to a survival advantage amidst the stress experienced under standard cell culture conditions. It is known that hESCs will readily undergo apoptosis when faced with stress (Liu et al., 2013), particularly through anoikis (Wang et al., 2009; Watanabe et al., 2007). Anoikis occurs early in apoptosis when cells become detached from their extracellular matrix before ultimately undergoing programmed cell death (Paoli et al., 2013). To measure whether WT cells undergo increased cell death compared with *MSH2* KO cells, we counted floating cells from WT and *MSH2* KO clones over a 2-day period. We found that the *MSH2* KO lines had significantly fewer floating cells compared with the WT line for H1 and YK26 cells (Figures 2A and 2B). To verify that floating cells were undergoing apoptosis, we performed a live/dead assay using annexin V and PI. We found that more than 98% of

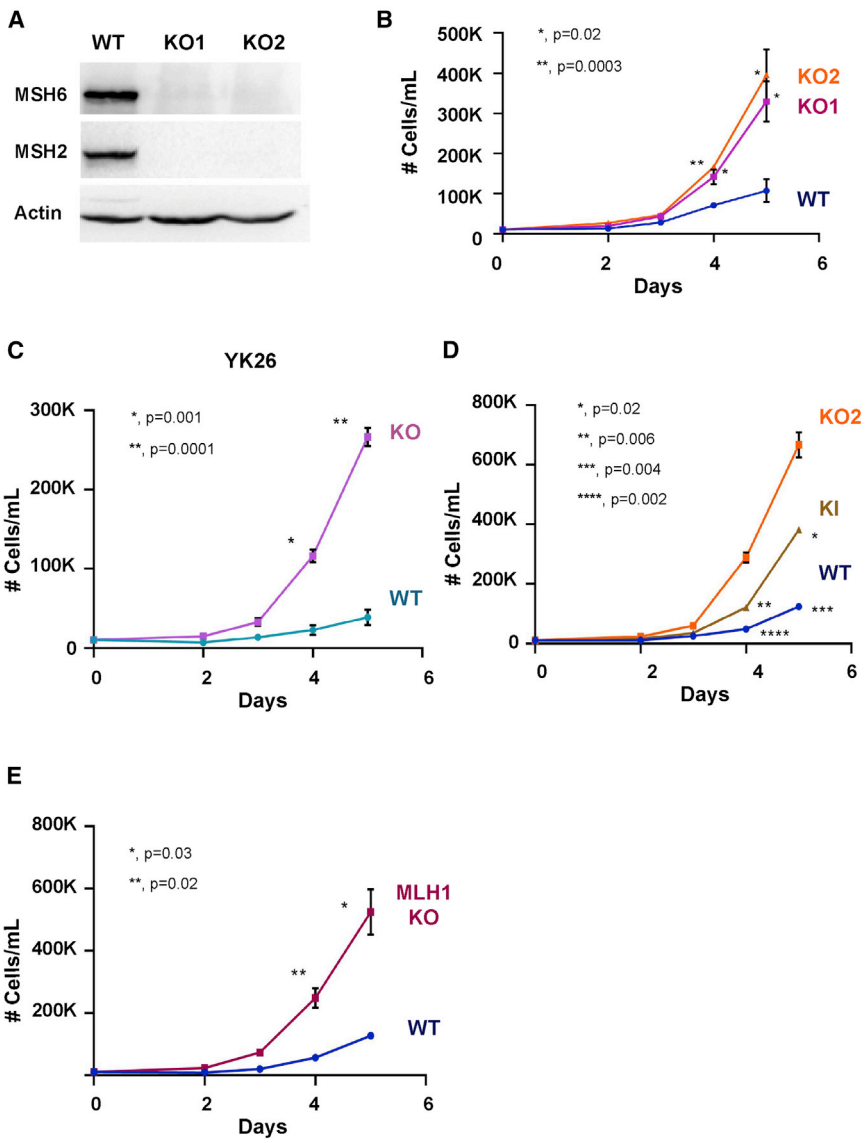

Figure 1. Loss of MMR in stem cells elicits an apparent growth advantage

(A) Western blot displaying loss of MSH2 and MSH6 expression in two independent *MSH2* knockout (KO) clones created in H1 human embryonic stem cells (hESCs). Actin is a loading control.

(B and C) Representative growth curves of H1 WT hESCs (B) and YK26 iPSCs (C) and corresponding *MSH2* KO clones.

(D) Representative growth curve comparing an *MSH2* KO clone and a version in which both *MSH2* alleles were restored to the WT sequence (KI).

(E) Representative growth curve comparing an *MLH1* KO clone with H1 WT hESCs.

Each experiment in (B)–(E) was performed in triplicate with 3 independent repeats. Two-tailed Student's t test was used to determine p values.

the floating cells were annexin V-positive or annexin V-and PI-positive in the WT and KO cell lines, indicating that they underwent apoptosis (Figure S3A). The viability of the floating cells was confirmed when replated floating cells were grown for 1 week and stained with methylene blue to observe colony formation. We found that less than 0.1% of the cells were able to re-form colonies (Figure S3B). We next examined whether the *MSH2* KO cells were less prone to apoptosis in general because of changes in levels of the apoptosis-regulating proteins BCL1 or PUMA but found that these protein levels are similar as in WT cells (Figure S3C). We also determined that the levels of OCT4, a marker for pluripotency (Boyer et al., 2005; Hay et al., 2004), were similar between WT and *MSH2* KO cells (Figures S3C and S3D). To determine whether the observed survival advantage in *MSH2* KO cells was due to direct loss of MMR and not a downstream mutation, we repeated the anoikis experiments with the *MSH2* KI line. The KI line had a significant increase in the percentage of floating cells compared with its parental *MSH2* KO clone, more like WT hESCs (Figure 2C). These data suggest that MSH2-deficient cells gain a survival advantage over WT cells, likely underlying the observed growth advantage.

MMR can induce a replication stress response in hESCs in the absence of exogenous stress

We have shown previously that, when an exogenous DNA-damaging agent is added to MMR-proficient hESCs, they undergo apoptosis marked by increased signs of replication stress and DNA double-strand breaks (DSBs) in an

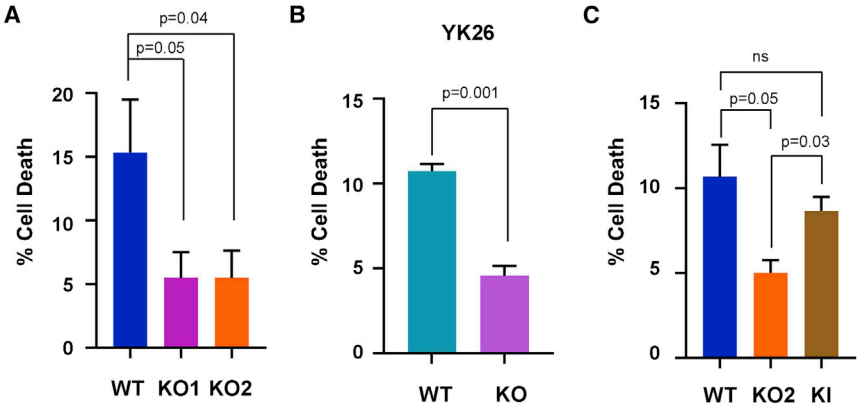

Figure 2. MMR-deficient stem cells are less likely to undergo anoikis

(A–C) Percentage of floating cells counted after 48 h for WT and *MSH2* KO clones (KO1 and KO2) (A), WT and *MSH2* KO YK26 cells (B), and WT, KO2, and a clone in which both *MSH2* alleles were restored to the WT sequence (KI) (C). Two-tailed Student's t test was used to determine p values. n = 3 independent repeats for all experiments.

MSH2-dependent manner (Gupta et al., 2018). Based on these findings, we wanted to determine whether the decreased cell death observed in *MSH2* KO cells under standard cell culture conditions was also accompanied by a decrease in markers of replication stress and DSB formation. To test this, we stained our cells with the general replication stress and DSB marker γH2AX. We observed that there were significantly more WT cells with γH2AX foci compared with *MSH2* KO cells (Figure 3A). We also stained the cells for the DSB markers 53BP1 and RAD51, which are involved in non-homologous end joining repair and homologous recombination repair, respectively. In line with the findings for γH2AX, we found significantly more WT cells with 53BP1 foci and RAD51 foci compared with *MSH2* KO cells (Figures 3B and 3C). These results indicate that WT hESCs grown under standard cell culture conditions show signs of low-level replication stress and DSBs that may ultimately lead to some cell death in an MMR-dependent manner.

Oxidative stress contributes to *MSH2* KO selective advantage

Our results suggest that hESCs grown under standard cell culture conditions experience low levels of stress that may increase MMR activity, resulting in activation of a DNA damage response. We hypothesized that one possible source of stress is oxidative damage because of cell culture at ambient oxygen levels. Oxidative stress can result in 8-oxoguanine lesions, which have been shown to activate the MMR pathway (Mazurek et al., 2002). We first wanted to assess how hESCs respond to oxidative stress because previous studies in other cell types have generated discordant results. Although some labs have reported that MMR-deficient cells are more resistant to oxidative damage (DeWeese et al., 1998; Glaab et al., 2001; Hardman et al., 2001), others have shown that MMR-deficient cells are more sensitive (Martin et al., 2009, 2010; Wang et al., 2005). To verify how hESCs respond to oxidative damage, we treated cells with increasing concentrations of the oxidative agent $KBrO_3$. We found that *MSH2* KO cells were more resistant to $KBrO_3$ compared with WT cells (Figure 4A). The *MSH2* KI line regained sensitivity to $KBrO_3$, similar to the WT hESC line (Figure S4A). These data support our prediction that WT hESCs are sensitive to oxidative damage and that low-level oxidative stress resulting from standard cell culture at 20% O_2 could be a potential driver of increased cell death in WT hESCs. To address this hypothesis, we attempted to reduce the level of WT cell death by decreasing oxidative stress. We treated our cells with the antioxidant vitamin C for 48 h and repeated our anoikis assay. We found that, when WT cells were treated with 75 μM vitamin C, there was a significant decrease in the percentage of cell death compared with *MSH2* KO cells (Figure 4B). Treatment with a second antioxidant, N-acetyl cysteine (NAC), at 250 μM for 48 h produced a similar result (Figure 4C). Finally, we repeated the assay with cells incubated in 5% O_2 to determine whether growing cells at reduced oxygen levels would affect cell survival. We found a significant decrease in cell death in our WT cells at 5% O_2, comparable with the KO lines (Figure 4D). Because a previous study indicated that growth of HCT-116 cancer cells under hypoxic conditions led to downregulation of MSH2 levels (Koshiji et al., 2005), we tested whether the reduction in cell death we observed under reduced oxygen conditions was instead due to loss of MSH2 protein. We found that growth of WT hESCs for 72 h at 5% O_2 did not alter MSH2 or MSH6 protein levels (Figure S4B). These results suggest that WT hESCs have an MMR-dependent sensitivity to even low levels of oxidative stress that could give rise to a survival advantage upon *MSH2* loss.

MMR-deficient colonic organoids have a growth and survival advantage

We next wanted to determine whether loss of MMR leads to a survival advantage in a more differentiated cell type.

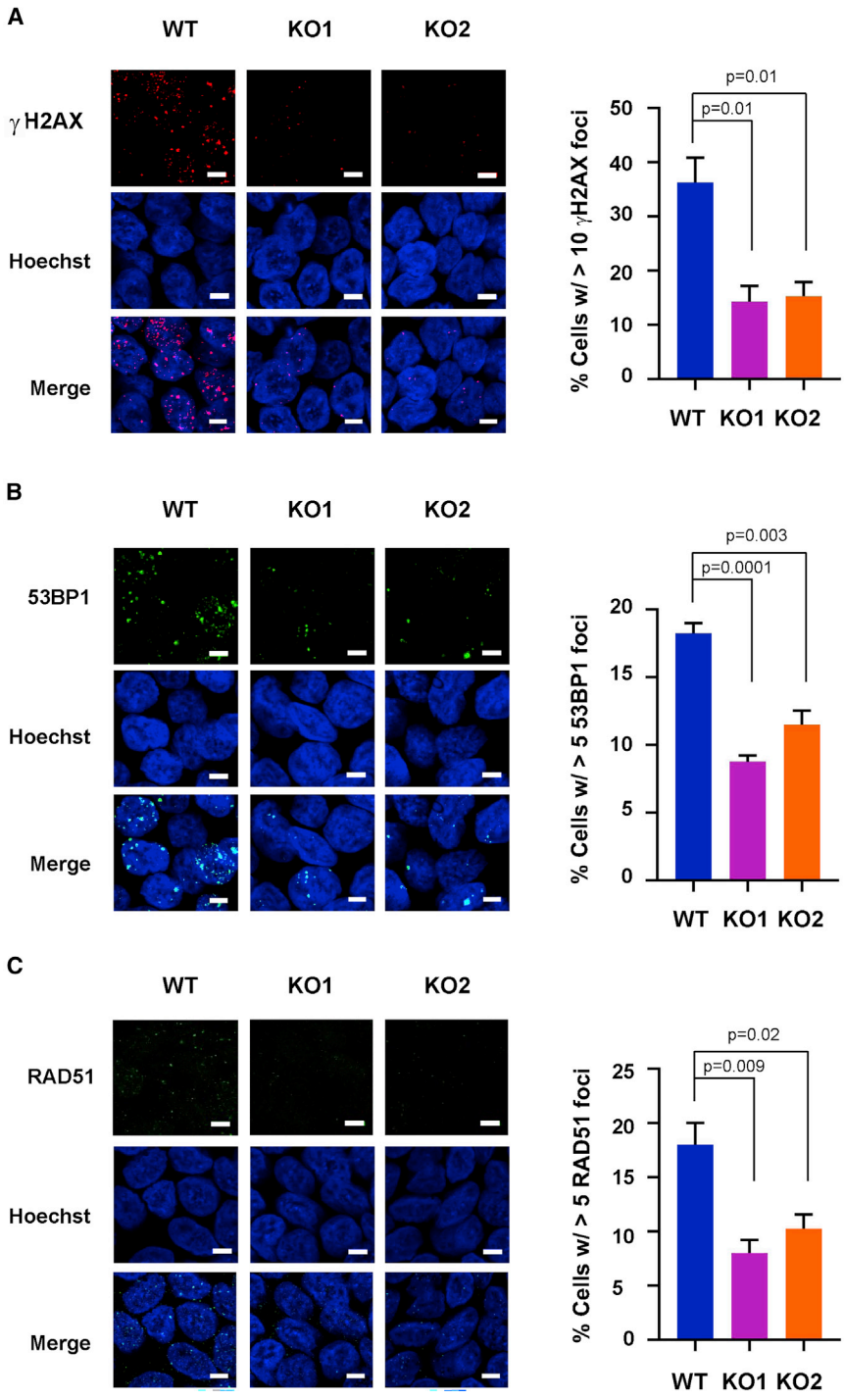

Figure 3. MMR-deficient hESCs display reduced DNA damage markers

(A–C) Immunofluorescence images of γH2AX foci (A), 53BP1 foci (B), and RAD51 foci (C) in wild-type (WT) and two *MSH2* KO hESC clones (KO1 and KO2) and quantitation of these results. Scale bars, 5 μm. Two-tailed Student's t test was used to determine p values. n = 3 independent repeats for all experiments.

The main form of cancer LS patients develop is colorectal cancer (Lynch et al., 2015), and it is believed that the colonic stem cell is the cell type from which cancer originates (Barker et al., 2009). We therefore examined the effects of *MSH2* loss in human colonic organoids (COs). To investigate this, we differentiated WT and *MSH2* KO hESCs into COs (Figures 5A and S5) and tracked their survival over a 2-week period. To confirm that any effects were due to loss of MMR function and not downstream mutations in those cells, we also differentiated the *MSH2* KI hESCs. We found that the *MSH2* KO hESCs consistently formed more colonic spheroids upon

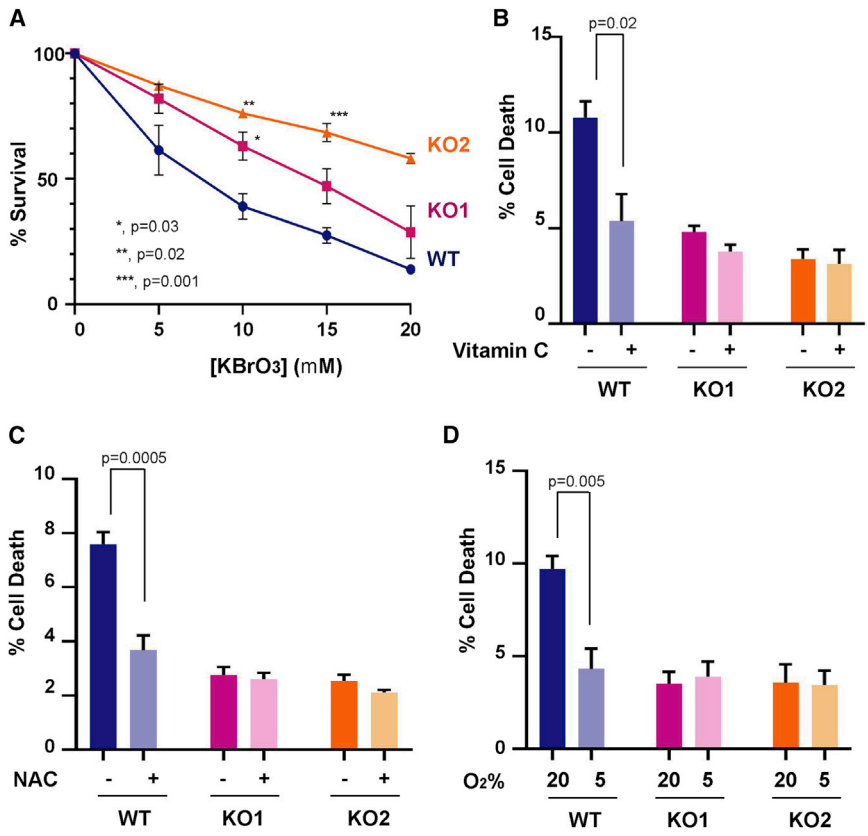

Figure 4. Oxidative damage contributes to the survival advantage in MMR-deficient hESCs

(A) Cell survival for WT and two *MSH2* KO hESC clones (KO1 and KO2) after 1-h treatment with increasing concentrations of the oxidative agent $KBrO_3$.

(B and C) Percentage of floating WT, KO1, and KO2 hESCs with or without 75 μM vitamin C (B) or 250 μM NAC (C) treatment for 48 h.

(D) Percentage of floating WT, KO1, and KO2 hESCs after growth at 20% or 5% O_2 for 72 h. Two-tailed Student's t test was used to determine p values. n = 3 independent repeats for experiments in (A), (B), and (D). For (C), n = 5 for WT, n = 4 for KO1, and n = 3 independent repeats for KO2.

completion of the differentiation protocol than the WT or KI hESCs (Figure 5B). We also found significantly fewer surviving WT and KI COs after 2 weeks (after normalizing for the starting number of COs) compared with *MSH2* KO COs (Figure 5C). While tracking survival, we noticed that the *MSH2* KO COs grew significantly larger than the WT and KI COs and were marked by increased budding, indicative of increased, localized stem cell proliferation (Sato et al., 2009, 2011; Yip et al., 2018; Figures 5A and 5D). These data suggest that even in a more differentiated, three-dimensional model system, loss of MMR function can confer a selective advantage.

DISCUSSION

Loss of MMR likely has an indirect effect on tumorigenesis through the mutator phenotype (Fishel and Kolodner, 1995). An increased mutation rate in an MMR-deficient cell would enhance the likelihood of a downstream mutation that affords that cell a selective advantage. However, we have proposed previously that loss of MMR may play a larger role in promoting tumorigenesis because of its role in mediating cell cycle arrest and apoptosis in response to certain forms of DNA damage (Heinen et al., 2002; Hollenbach et al., 2011). In this study, we used hESCs in which the *MSH2* gene was disrupted by CRISPR gene editing to show that loss of MMR function results in an immediate survival advantage even in the absence of added exogenous DNA-damaging agents. We also showed that this phenotype could be rescued upon restoring MSH2 expression in the KO cells. We demonstrated that cells lacking MSH2 form COs more efficiently, marked by enhanced survival and size. These *MSH2* KO COs displayed increased budding, representative of sites of increased intestinal stem cell activity in organoids (Sato et al., 2009, 2011; Yip et al., 2018). This result suggests that loss of MMR provides a direct selective advantage to colonic stem cells as well, indicating the potential for a role of the MMR-dependent damage response in preventing tumorigenesis.

This damage response has been implicated as a mechanism of chemotherapeutic resistance in MMR-deficient tumors. Alkylating agents, 5-fluorouracil, cisplatin, and other DNA-damaging agents that elicit an MMR-dependent damage response in cell culture models are less effective in treating MMR-deficient tumors (Gupta and Heinen, 2019; Heinen, 2014). However, a role of the MMR-dependent damage response in preventing tumorigenesis has largely been underexplored. Evidence from animal models support a role of the MMR-dependent damage response in tumor

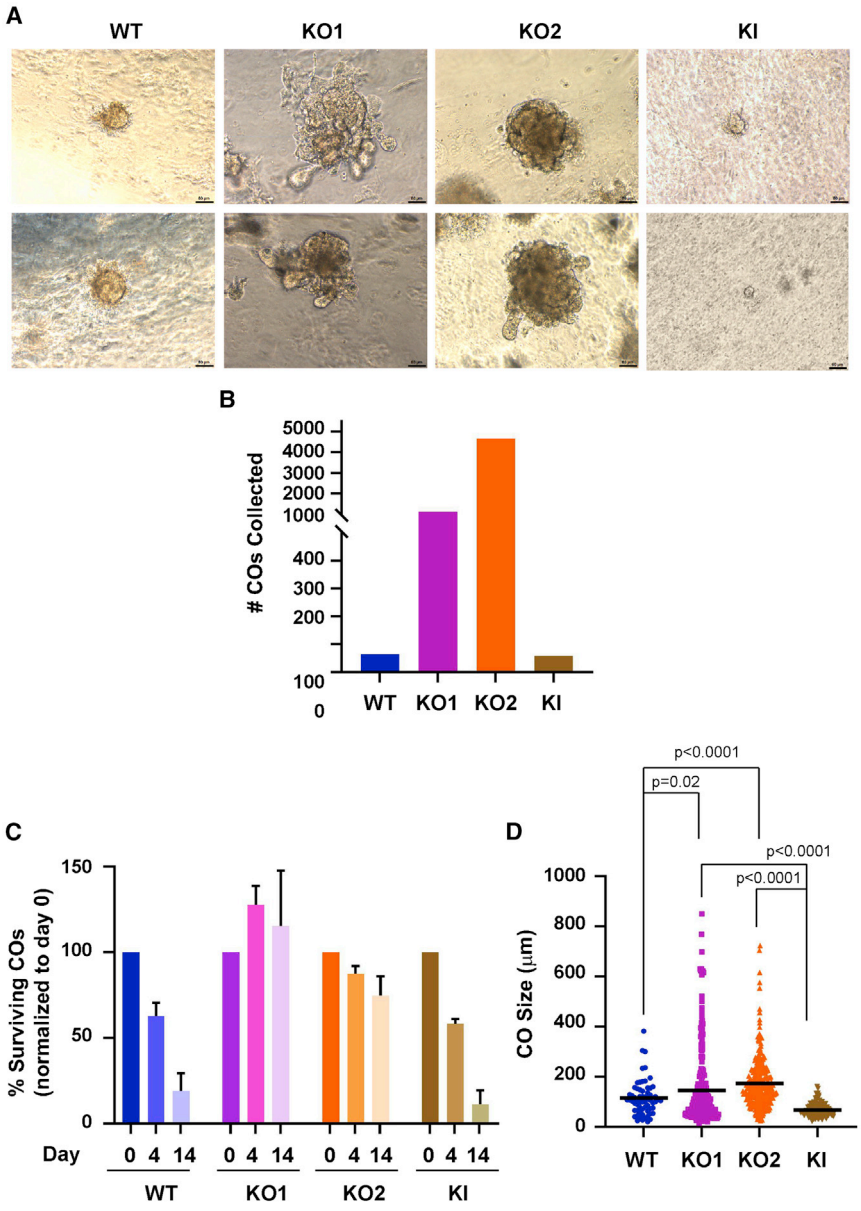

Figure 5. MMR-deficient hESCs are more proficient at forming COs

WT, *MSH2* KO (KO1 and KO2), and KO2 hESCs in which both alleles of the *MSH2* sequence were restored (KI) were differentiated into colonic organoids (COs) and imaged using light microscopy. Scale bars, 80 μm.

(A) Two representative images of WT, KO1, KO2, and KI COs.

(B) Total number of WT, KO1, KO2, and KI COs collected during a representative differentiation experiment.

(C) Total WT, KO1, KO2, and KI COs in a Matrigel plug on days 0, 4, and 14 after differentiation, normalized to the count on day 0. n = 3 for WT and KO1, n = 2 independent repeats for KO2 and KI.

(D) Diameter of WT (n = 63), KO1 (n = 258), KO2 (n = 333), and KI (nN = 125) COs, measured on day 4 after differentiation. Two-tailed Student's t test was used to determine p values.

suppression. Mouse models with point mutations in *Msh2* or *Msh6* have been described that disrupt MMR repair activity but leave the DNA damage response intact (Lin et al., 2004; Yang et al., 2004). Although these animals still develop tumors, onset of tumorigenesis is delayed compared with MMR gene KO mice, suggesting that both MMR functions may affect cancer development. In a mosaic mouse model with a mix of intestinal MMR-proficient and -deficient cells, the DNA alkylating agent temozolomide led to an increase in entirely MMR-deficient crypts, indicating that DNA damage stress creates a selection pressure for MMR-deficient stem cells (Wojciechowicz et al., 2014). Tumorigenesis in these animals is also accelerated, consistent with a model where increased numbers of MMR-deficient cells can spur tumorigenesis.

By examining MMR loss in hESCs, we could test the effects of MMR deficiency in a non-cancerous human stem cell line that had not accumulated multiple mutations and undergone rounds of selection and expansion. Our previous work found that treatment of hESCs with an alkylating agent leads to increased MMR activity, resulting in replication stress, DSBs, and apoptosis (Gupta et al., 2018; Lin et al., 2014). However, the immediate growth advantage we observed in this study in MMR-deficient hESCs in the absence of any exogenous DNA-damaging agents was unexpected. We determined that the MMR-deficient cells

did not proliferate faster but acquired a survival advantage, consistent with loss of the MMR-dependent damage response. However, because we did not treat the cells with any DNA-damaging agents, we hypothesized that WT cells may be responding to oxidative stress from the high ambient levels of oxygen under standard cell culture conditions. Conflicting responses to oxidative damage in MMR-proficient versus -deficient cells have been reported. Early studies demonstrated that loss of MMR function leads to decreased repair of 8-oxoguanine lesions caused by gamma irradiation or H_2O_2 and decreased apoptosis (DeWeese et al., 1998; Glaab et al., 2001; Hardman et al., 2001; Wang et al., 2005). Conversely, a more recent study has shown that cancer cells with restored MMR function are more sensitive to agents that cause oxidative stress, including methotrexate and menadione (Martin et al., 2009). The same group later showed that deficient MMR is in a synthetic lethal relationship with loss of DNA polymerases involved in repairing oxidative lesions, consistent with the model where increased 8-oxoguanine lesions increase cell death in MMR-deficient cells (Martin et al., 2010). The reasons behind these opposing findings are not clear. The source of oxidative stress used may partially underlie the disparate results because different agents may have more extensive effects beyond just oxidative stress, such as methotrexate, which interferes with folate metabolism. The levels of induced oxidative damage may also affect the response because studies reporting increased resistance of MMR-deficient cells to H_2O_2 used higher doses (Glaab et al., 2001; Hardman et al., 2001). There is also the suggestion that the effect may depend on the MMR gene that is depleted. The early studies showed increased resistance of *MLH1*-deficient cells to oxidative stress (Glaab et al., 2001; Hardman et al., 2001), whereas Martin et al. (2009) showed decreased resistance of MMR-deficient cells focused on *MSH2*. However, our experiments primarily utilized *MSH2* KO hESCs, finding them more resistant to oxidative stress caused by $KBrO_3$. We found that antioxidants provided protection to MMR-proficient WT cells growing under standard cell culture conditions. Our results suggest a role of MMR in response to 8-oxoguanine lesions that is similar to the MMR-dependent response to O^6-methylguanine lesions, in which active MMR is required to signal the presence of damage.

Our results in hESCs and differentiated COs support the *in vivo* observations indicative of an effect of the MMR-dependent damage response on tumorigenesis described above. Future studies will be important to determine whether a survival advantage is gained from MMR loss in human adult stem cells. Loss of the remaining WT MMR gene allele in a colonic stem cell in a patient with LS, for example, may cause that cell to gain a selective advantage over its heterozygous neighbors. This may be an important step in tumorigenesis by establishing a field of MMR-deficient cells from which a tumor could emerge. Although this model presupposes that loss of MMR function is an early step in tumorigenesis, this is not a settled question. One study examining colorectal polyps in patients with LS found that microsatellite instability, a marker for defective MMR, was present in only half of polyps, with an increased prevalence in larger adenomas, suggesting that loss of MMR function is a later event in tumorigenesis (Yurgelun et al., 2012). In contrast, a second study demonstrated that loss of MMR could be identified in over 70% of polyps from patients with LS, including 100% of adenomas with high-grade dysplasia, suggesting that loss of MMR is a frequent event even in these pre-cancerous lesions (Walsh et al., 2012). The presence of histologically normal colonic crypts that lack MMR protein expression in normal mucosa from patients with LS implicates loss of MMR as a very early event (Kloor et al., 2012; Lee et al., 2022; Pai et al., 2018; Staffa et al., 2015). These studies identified MMR-deficient foci that ranged in size from a single crypt to poly-cryptic foci as large as 49 crypts. These poly-cryptic foci, sometimes marked by increased crypt branching and fission, suggest that a single MMR-defective stem cell could expand into clonal fields of MMR-deficient cells from which a tumor could arise. In conjunction with our results, we propose that loss of the MMR-dependent damage response in a single colonic stem cell creates a selective advantage, leading to clonal expansion and creation of these observed MMR-deficient colonic crypts.

The exciting aspect of this prediction is that, if we can understand the environmental exposures that result in the selective pressures driving expansion of MMR-deficient cells, then we could intervene to prevent this and, thus, reduce tumorigenesis. One exposure that is a known risk factor for cancer in patients with LS is smoking (Brand et al., 2006; Diergaarde et al., 2007; Pande et al., 2010; Watson et al., 2004; Winkels et al., 2012), which results in exposure of colonic cells to a number of genotoxic compounds such as polycyclic aromatic hydrocarbons, *N*-nitrosamines, and various free radicals and oxidants that cause increased oxidative stress (Godschalk et al., 2002). Persistent oxidative stress can also arise from chronic inflammation (Todoric et al., 2016), another potential risk factor for cancer in patients with LS. Co-occurrence of inflammatory bowel disease in patients with LS results in an earlier age of colorectal cancer onset (Derikx et al., 2017). Nearly two-thirds of ulcerative colitis-associated CRCs are marked by defective MMR at an early stage (Heinen et al., 1997; Ishitsuka et al., 2001; Suzuki et al., 1994; Tahara et al., 2005). Long-term exposure to these sources of stress could provide selective pressure for loss of MMR. Lifestyle changes or chemopreventative approaches, such as antioxidants and anti-inflammatories, might dampen the advantage gained by MMR loss, increasing the chances

that an MMR-deficient cell is outcompeted in the niche by other MMR-proficient stem cells. This outcome would reduce disease penetrance in patients with LS. Consistent with this prediction, aspirin, a non-steroidal anti-inflammatory drug (NSAID), reduces long-term CRC incidence in patients with LS (Burn et al., 2011, 2020). Our findings that MMR-deficient stem cells acquire a selective advantage over WT cells provides important mechanistic insight that could be exploited in future translational studies to reduce the risk of cancer prevalence in patients with LS.

EXPERIMENTAL PROCEDURES

Resource availability

Corresponding author

The corresponding author is C.D.H. (email: cheinen@uchc.edu; telephone: 860-679-8859).

Materials availability

All cell lines generated for this study are available upon request.

Cell culture

H1 hESCs obtained from the WiCell Research Institute were cultured under feeder-free conditions in PeproGrow hESC medium (PeproTech) at 37°C and 5% CO_2. YK26 iPSCs were reprogrammed from human dermal fibroblasts as described previously (Zeng et al., 2010). *MSH2* KO hESC lines were derived previously (Gupta et al., 2018; Rath et al., 2019). Cell lines were passaged using StemPro Accutase Cell Dissociation Reagent (Gibco) every 4–5 days onto tissue culture plates coated with growth factor-reduced Matrigel (Corning) in the presence of ROCK (Rho kinase) inhibitor. The following day, hESC medium was replaced with fresh medium without ROCK inhibitor. All experiments took place 3–4 days after initial seeding of cells, except for the growth analysis and DNA damage experiments. For growth analysis experiments, 5,000 cells/well of a 24-well tissue culture plate were seeded (day 0). Starting on day 2, hESCs were harvested and counted using a hemocytometer. hESCs were harvested and counted for 3 more consecutive days. Each experiment was performed three times and consisted of three technical replicates each.

Cell cycle analysis

Cell doubling times were determined as described previously (Becker et al., 2006). Briefly, WT and MSH2 KO hESCs were seeded and expanded for 3 days. hESCs were incubated with 3 mg/mL CFSE (Sigma) dissolved in PBS with Ca^{2+} and Mg^{2+} for 10 min at 37°C. Cells were then harvested every 24 h for 72 h. The cells were fixed with 4% paraformaldehyde (PFA) for 10 min at room temperature (RT), washed twice with PBS, resuspended in 500 μL of PBS, and filtered before being analyzed using an LSRII flow cytometer (BD Biosciences). The data were analyzed using FlowJo, and the mean CSFE value was compared with the time 0 value to determine the rate of decay for each 24-h time period. To analyze cell cycle profiles, equal numbers of WT and *MSH2* KO hESCs were incubated at 37°C with 10 μM 5-ethynyl-2′-dexoyuridine (EdU) for 30 min. Cells were then washed and harvested before being fixed with 4% PFA for 15 min. EdU incorporation was detected using the Click-iT Plus EdU Alexa Fluor 647 Flow Cytometry Assay Kit (Molecular Probes). Cells were stained with Hoechst-33342 (Life Technologies) for 10 min at RT and filtered before being analyzed using an LSRII flow cytometer. Data were analyzed using FlowJo.

Immunofluorescence and image analysis

hESCs were seeded onto Matrigel-coated Thermanox Cell Culture Coverslips (Nunc). Cells were washed once and fixed with 4% PFA for 10 min at RT. Cells were then permeabilized with 1% Triton X-100 for 10 min, washed with PBS, and blocked with 3% goat serum in PBS for 1 h at RT. Cells were incubated with primary antibodies diluted in 3% goat serum for 1–2 h at RT and then with secondary antibodies diluted in 3% goat serum for 1 h at RT (Alexa Fluor 488 or Alexa Fluor 568, Molecular Probes). Primary antibodies used included γH2AX (05-636, EMD Millipore), 53BP1 (NB100-304, Novus Biologicals), RAD51 (PC130, EMD Millipore), and OCT4 (19857, Abcam). The nuclei of cells were stained using Hoechst-33342 for 10 min at RT. Coverslips were mounted and imaged using a Carl Zeiss Plan-apochromat 63×/1.4 numerical aperture oil immersion objective on a Carl Zeiss LSM 780 confocal microscope. Images were analyzed using MetaMorph.

MTT survival assays

hESCs were seeded onto Matrigel-coated wells of a 24-well tissue culture plate. Cells were treated with increasing concentrations of $KBrO_3$ in PBS with Ca^{2+} and Mg^{2+} to induce oxidative damage for 1 h or increasing concentrations of MNNG for 48 h as described previously (Rath et al., 2019). Cells were washed, replaced with fresh medium, and incubated for 16 or 24 h. Cell viability was assessed using Vybrant MTT (3-(4,5-dimethylthiazol-2-yl)-2,5-diphenyltetrazolium bromide tetrazolium) Cell Proliferation Assay Kit (V-13154) according to the manufacturer's instructions.

Cell death assay

hESCs were seeded onto Matrigel-coated wells of a 6-well tissue culture plate. Adherent cells from 3 wells were counted the next day, and the average value was used as the baseline cell number (day 1). The remaining wells of hESCs were washed once with PBS, given fresh medium, and incubated for 48 h. On day 3, the floating and adherent cells were collected separately from each well and counted. The following equation was used to determine the percentage of cell death for each well:

percent cell death = [number of floating cells/(number of adherent cells on day 3 – average baseline cell number on day 1)] × 100.

To verify that the floating cells underwent apoptosis, cells were stained with annexin and PI as indicated in the Alexa Fluor 488 Annexin V/Dead Cell Apoptosis Kit with Alexa

Fluor 488 Annexin V and PI for Flow Cytometry protocol (Invitrogen). Cell death was also confirmed by staining cells with methylene blue to determine the number of floating cells that could re-form colonies. For antioxidant experiments, cells were treated with 75 μM vitamin C or 250 μM NAC the day after the cells were seeded and incubated for 48 h. For experiments in reduced oxygen, cells were plated and incubated at 20% or 5% O_2. Fresh medium was added after 24 h, and floating cells were collected after

an additional 48 h. Floating and adherent cells were harvested and counted as described above.

Western blots

hESCs were harvested, and total cell extracts were obtained as described previously (Gupta et al., 2018). Equal concentrations of protein were loaded onto an SDS-PAGE gel and transferred to a polyvinylidene fluoride (PVDF) membrane. Western blot analysis was performed using the following antibodies: MSH2 (NA27, EMD Millipore), MLH1 (550838, BD Biosciences), MSH6 (A300-023A, Bethyl Laboratories), PMS2 (556415; Santa Cruz Biotechnology), BCL-2 (SC-7382, Santa Cruz), Actin (SC-8432, Santa Cruz), and PUMA (12450T, Cell Signaling Technology).

Gene targeting

Single-cell dilution seeding of *MSH2* KO cells (KO2) was used to isolate single-cell clones. Genomic DNA for each clone was collected and PCR amplified using high-fidelity Phusion DNA polymerase (New England Biolabs), and Sanger sequencing was completed. Sequencing results were entered into the ICE (Inference of CRISPR Edits) Analyzer on ice.synthego.com, which provided computational analysis, showing the alleles present in each clonal sample. Results for a single clone that presented only two alleles were used for the *in silico* design (CRISPOR) (Concordet and Haeussler, 2018) of a single guide RNA (sgRNA) for each allele and a single-stranded oligodeoxyribonucleotide (ssODN) for transfection into the *MSH2* KO clone (Table S1). Transfected cells were treated with 1 μg/mL of puromycin for 2 days and then given 1× CloneR (STEMCELL Technologies) for 5 days to isolate single-cell-derived clones. Genomic DNA was isolated from clones, PCR amplified using high-fidelity Phusion DNA polymerase (NEB), and genotyped using Sanger sequencing. KO of *MSH2* in YK26 iPSCs was performed as described previously (Rath et al., 2019) with the appropriate sgRNA (Table S1).

Organoid formation

hESCs were differentiated as described previously (Múnera et al., 2017). Briefly, hESC medium was removed from the cells and replaced with RPMI 1640 + L-glutamine, non-essential amino acids, 100 ng/mL Activin-A (Cell Guidance Systems), and 15 ng/mL BMP4 (Gibco) for 24 h. This was followed by the same medium without BMP4 but with addition of 0.2% fetal bovine serum (FBS) for 1 day and then 2% FBS for an additional day. On day 4 of the differentiation protocol, the cells were incubated in RPMI 1640 + L-glutamine, 2% FBS, non-essential amino acids, 3 μM CHIR99021 (Selleck Chemicals), and 500 ng/mL FGF-4 (R&D Systems) for 4 days. Floating spheroids were harvested and placed into Matrigel in DMEM-F12 + L-glutamine, B27 (Gibco), N2 (Gibco), 100 ng/mL epidermal growth factor (EGF; R&D Systems), and 100 ng/mL BMP2 (R&D Systems) for 3 days. After 3 days, BMP2 was removed from the basal medium, and organoids were counted to determine the number of starting organoids (day 0) and again on days 4 and 14. The number of organoids counted on days 4 and 14 were normalized to day 0. On day 4, the diameter of each organoid was measured at the widest point of the organoid to determine size. Organoids were imaged using an Olympus IX50 light microscope and analyzed using Q-Imaging software.

DATA AND CODE AVAILABILITY

All data are available upon reasonable request.

SUPPLEMENTAL INFORMATION

Supplemental information can be found online at https://doi.org/10.1016/j.stemcr.2022.10.009.

AUTHOR CONTRIBUTIONS

K.M.-H. conceived the project, conducted experiments, analyzed the data, and wrote the manuscript. D.G. conceived the project and conducted experiments. A.A.R., C.G., and A.R. conducted experiments. C.D.H. conceived the project, analyzed the data, funded the research, and wrote the manuscript. All authors reviewed and edited the manuscript.

ACKNOWLEDGMENTS

We acknowledge Elizabeth Szabo for technical help. This work was supported by NIH grants CA245514 and CA222477.

CONFLICT OF INTERESTS

The authors declare no competing interests.

Received: March 4, 2022
Revised: October 11, 2022
Accepted: October 12, 2022
Published: November 10, 2022

REFERENCES

Aebi, S., Kurdi-Haidar, B., Gordon, R., Cenni, B., Zheng, H., Fink, D., Christen, R.D., Boland, C.R., Koi, M., Fishel, R., and Howell, S.B. (1996). Loss of DNA mismatch repair in acquired resistance to cisplatin. Cancer Res. *56*, 3087–3090.

Barker, N., Ridgway, R.A., van Es, J.H., van de Wetering, M., Begthel, H., van den Born, M., Danenberg, E., Clarke, A.R., Sansom, O.J., and Clevers, H. (2009). Crypt stem cells as the cells-of-origin of intestinal cancer. Nature *457*, 608–611.

Becker, K.A., Ghule, P.N., Therrien, J.A., Lian, J.B., Stein, J.L., van Wijnen, A.J., and Stein, G.S. (2006). Self-renewal of human embryonic stem cells is supported by a shortened G1 cell cycle phase. J. Cell. Physiol. *209*, 883–893.

Boyer, L.A., Lee, T.I., Cole, M.F., Johnstone, S.E., Levine, S.S., Zucker, J.P., Guenther, M.G., Kumar, R.M., Murray, H.L., Jenner, R.G., et al. (2005). Core transcriptional regulatory circuitry in human embryonic stem cells. Cell *122*, 947–956.

Brand, R.M., Jones, D.D., Lynch, H.T., Brand, R.E., Watson, P., Ashwathnayaran, R., and Roy, H.K. (2006). Risk of colon cancer in hereditary non-polyposis colorectal cancer patients as predicted by fuzzy modeling: influence of smoking. World J. Gastroenterol. *12*, 4485–4491.

Burn, J., Gerdes, A.-M., Macrae, F., Mecklin, J.-P., Moeslein, G., Olschwang, S., Eccles, D., Evans, D.G., Maher, E.R., Bertario, L., et al. (2011). Long-term effect of aspirin on cancer risk in carriers

of hereditary colorectal cancer: an analysis from the CAPP2 randomised controlled trial. Lancet *378*, 2081–2087.

Burn, J., Sheth, H., Elliott, F., Reed, L., Macrae, F., Mecklin, J.-P., Möslein, G., McRonald, F.E., Bertario, L., Evans, D.G., et al. (2020). Cancer prevention with aspirin in hereditary colorectal cancer (Lynch syndrome), 10-year follow-up and registry-based 20-year data in the CAPP2 study: a double-blind, randomised, placebo-controlled trial. Lancet *395*, 1855–1863.

Carethers, J.M., Chauhan, D.P., Fink, D., Nebel, S., Bresalier, R.S., Howell, S.B., and Boland, C.R. (1999). Mismatch repair proficiency and in vitro response to 5-fluorouracil. Gastroenterology *117*, 123–131.

Concordet, J.-P., and Haeussler, M. (2018). CRISPOR: intuitive guide selection for CRISPR/Cas9 genome editing experiments and screens. Nucleic Acids Res. *46*, W242–W245.

Derikx, L.A.A.P., Smits, L.J.T., van Vliet, S., Dekker, E., Aalfs, C.M., van Kouwen, M.C.A., Nagengast, F.M., Nagtegaal, I.D., Hoogerbrugge, N., and Hoentjen, F. (2017). Colorectal cancer risk in patients with Lynch syndrome and inflammatory bowel disease. Clin. Gastroenterol. Hepatol. *15*, 454–458.e1.

DeWeese, T.L., Shipman, J.M., Larrier, N.A., Buckley, N.M., Kidd, L.R., Groopman, J.D., Cutler, R.G., te Riele, H., and Nelson, W.G. (1998). Mouse embryonic stem cells carrying one or two defective Msh2 alleles respond abnormally to oxidative stress inflicted by low-level radiation. Proc. Natl. Acad. Sci. USA *95*, 11915–11920.

Diergaarde, B., Braam, H., Vasen, H.F., Nagengast, F.M., van Muijen, G.N.P., Kok, F.J., and Kampman, E. (2007). Environmental factors and colorectal tumor risk in individuals with hereditary nonpolyposis colorectal cancer. Clin. Gastroenterol. Hepatol. *5*, 736–742.

Fink, D., Nebel, S., Aebi, S., Zheng, H., Cenni, B., Nehmé, A., Christen, R.D., and Howell, S.B. (1996). The role of DNA mismatch repair in platinum drug resistance. Cancer Res. *56*, 4881–4886.

Fishel, R. (2001). The selection for mismatch repair defects in hereditary nonpolyposis colorectal cancer. Cancer Res. *61*, 7369–7374.

Fishel, R. (2015). Mismatch repair. J. Biol. Chem. *290*, 26395–26403.

Fishel, R., and Kolodner, R.D. (1995). Identification of mismatch repair genes and their role in the development of cancer. Curr. Opin. Genet. Dev. *5*, 382–395.

Glaab, W.E., Hill, R.B., and Skopek, T.R. (2001). Suppression of spontaneous and hydrogen peroxide-induced mutagenesis by the antioxidant ascorbate in mismatch repair-deficient human colon cancer cells. Carcinogenesis *22*, 1709–1713.

Godschalk, R., Nair, J., van Schooten, F.J., Risch, A., Drings, P., Kayser, K., Dienemann, H., and Bartsch, H. (2002). Comparison of multiple DNA adduct types in tumor adjacent human lung tissue: effect of cigarette smoking. Carcinogenesis *23*, 2081–2086.

Goellner, E.M., Putnam, C.D., and Kolodner, R.D. (2015). Exonuclease 1-dependent and independent mismatch repair. DNA Repair *32*, 24–32.

Gupta, D., and Heinen, C.D. (2019). The mismatch repair-dependent DNA damage response: mechanisms and implications. DNA Repair *78*, 60–69.

Gupta, D., Lin, B., Cowan, A., and Heinen, C.D. (2018). ATR-Chk1 activation mitigates replication stress caused by mismatch repair-dependent processing of DNA damage. Proc. Natl. Acad. Sci. USA *115*, 1523–1528.

Hardman, R.A., Afshari, C.A., and Barrett, J.C. (2001). Involvement of mammalian MLH1 in the apoptotic response to peroxide-induced oxidative stress. Cancer Res. *61*, 1392–1397.

Hay, D.C., Sutherland, L., Clark, J., and Burdon, T. (2004). Oct-4 knockdown induces similar patterns of endoderm and trophoblast differentiation markers in human and mouse embryonic stem cells. Stem Cell. *22*, 225–235.

Heinen, C.D. (2014). Translating mismatch repair mechanism into cancer care. Curr. Drug Targets *15*, 53–64.

Heinen, C.D., Noffsinger, A.E., Belli, J., Straughen, J., Fischer, J., Groden, J., and Fenoglio-Preiser, C.M. (1997). Regenerative lesions in ulcerative colitis are characterized by microsatellite mutation. Genes Chromosomes Cancer *19*, 170–175.

Heinen, C.D., Schmutte, C., and Fishel, R. (2002). DNA repair and tumorigenesis: lessons from hereditary cancer syndromes. Cancer Biol. Ther. *1*, 477–485.

Hollenbach, J.P., Resch, A.M., Palakodeti, D., Graveley, B.R., and Heinen, C.D. (2011). Loss of DNA mismatch repair imparts a selective advantage in planarian adult stem cells. PLoS One *6*, e21808.

Ishitsuka, T., Kashiwagi, H., and Konishi, F. (2001). Microsatellite instability in inflamed and neoplastic epithelium in ulcerative colitis. J. Clin. Pathol. *54*, 526–532.

Kloor, M., Huth, C., Voigt, A.Y., Benner, A., Schirmacher, P., von Knebel Doeberitz, M., and Bläker, H. (2012). Prevalence of mismatch repair-deficient crypt foci in Lynch syndrome: a pathological study. Lancet Oncol. *13*, 598–606.

Kolodner, R. (1996). Biochemistry and genetics of eukaryotic mismatch repair. Genes Dev. *10*, 1433–1442.

Koshiji, M., To, K.K.-W., Hammer, S., Kumamoto, K., Harris, A.L., Modrich, P., and Huang, L.E. (2005). HIF-1a induces genetic instability by transcriptionally downregulating MutSalpha expression. Mol. Cell *17*, 793–803.

Kunkel, T.A., and Erie, D.A. (2005). DNA mismatch repair. Annu. Rev. Biochem. *74*, 681–710.

Lee, B.C.H., Robinson, P.S., Coorens, T.H.H., Yan, H.H.N., Olafsson, S., Lee-Six, H., Sanders, M.A., Siu, H.C., Hewinson, J., Yue, S.S.K., et al. (2022). Mutational landscape of normal epithelial cells in Lynch Syndrome patients. Nat. Commun. *13*, 2710.

Li, Z., Pearlman, A.H., and Hsieh, P. (2016). DNA mismatch repair and the DNA damage response. DNA Repair *38*, 94–101.

Lin, B., Gupta, D., and Heinen, C.D. (2014). Human pluripotent stem cells have a novel mismatch repair-dependent damage response. J. Biol. Chem. *289*, 24314–24324.

Lin, D.P., Wang, Y., Scherer, S.J., Clark, A.B., Yang, K., Avdievich, E., Jin, B., Werling, U., Parris, T., Kurihara, N., et al. (2004). An Msh2 point mutation uncouples DNA mismatch repair and apoptosis. Cancer Res. *64*, 517–522.

Liu, J.C., Guan, X., Ryan, J.A., Rivera, A.G., Mock, C., Agrawal, V., Agarwal, V., Letai, A., Lerou, P.H., and Lahav, G. (2013). High

mitochondrial priming sensitizes hESCs to DNA-damage-induced apoptosis. Cell Stem Cell *13*, 483–491.

Lynch, H.T., Snyder, C.L., Shaw, T.G., Heinen, C.D., and Hitchins, M.P. (2015). Milestones of Lynch syndrome: 1895-2015. Nat. Rev. Cancer *15*, 181–194.

Martin, S.A., McCabe, N., Mullarkey, M., Cummins, R., Burgess, D.J., Nakabeppu, Y., Oka, S., Kay, E., Lord, C.J., and Ashworth, A. (2010). DNA polymerases as potential therapeutic targets for cancers deficient in the DNA mismatch repair proteins MSH2 or MLH1. Cancer Cell *17*, 235–248.

Martin, S.A., McCarthy, A., Barber, L.J., Burgess, D.J., Parry, S., Lord, C.J., and Ashworth, A. (2009). Methotrexate induces oxidative DNA damage and is selectively lethal to tumour cells with defects in the DNA mismatch repair gene MSH2. EMBO Mol. Med. *1*, 323–337.

Mazurek, A., Berardini, M., and Fishel, R. (2002). Activation of human MutS homologs by 8-Oxo-guanine DNA damage. J. Biol. Chem. *277*, 8260–8266.

Modrich, P. (2006). Mechanisms in eukaryotic mismatch repair. J. Biol. Chem. *281*, 30305–30309.

Múnera, J.O., Sundaram, N., Rankin, S.A., Hill, D., Watson, C., Mahe, M., Vallance, J.E., Shroyer, N.F., Sinagoga, K.L., Zarzoso-Lacoste, A., et al. (2017). Differentiation of human pluripotent stem cells into colonic organoids via transient activation of BMP signaling. Cell Stem Cell *21*, 51–64.e6.

Pai, R.K., Dudley, B., Karloski, E., Brand, R.E., O'Callaghan, N., Rosty, C., Buchanan, D.D., Jenkins, M.A., Thibodeau, S.N., French, A.J., et al. (2018). DNA mismatch repair protein deficient non-neoplastic colonic crypts: a novel indicator of Lynch syndrome. Mod. Pathol. *31*, 1608–1618.

Pande, M., Lynch, P.M., Hopper, J.L., Jenkins, M.A., Gallinger, S., Haile, R.W., LeMarchand, L., Lindor, N.M., Campbell, P.T., Newcomb, P.A., et al. (2010). Smoking and colorectal cancer in Lynch syndrome: results from the colon cancer family registry and the university of Texas M.D. Anderson cancer center. Clin. Cancer Res. *16*, 1331–1339.

Paoli, P., Giannoni, E., and Chiarugi, P. (2013). Anoikis molecular pathways and its role in cancer progression. Biochim. Biophys. Acta *1833*, 3481–3498.

Pluciennik, A., Dzantiev, L., Iyer, R.R., Constantin, N., Kadyrov, F.A., and Modrich, P. (2010). PCNA function in the activation and strand direction of MutL endonuclease in mismatch repair. Proc. Natl. Acad. Sci. USA *107*, 16066–16071.

Rath, A., Mishra, A., Ferreira, V.D., Hu, C., Omerza, G., Kelly, K., Hesse, A., Reddi, H.V., Grady, J.P., and Heinen, C.D. (2019). Functional interrogation of Lynch syndrome associated MSH2 missense variants via CRISPR-Cas9 gene editing in human embryonic stem cells. Hum. Mutat. *40*, 2044–2056.

Rath, A., Radecki, A.A., Rahman, K., Gilmore, R.B., Hudson, J.R., Cenci, M., Tavtigian, S.V., Grady, J.P., and Heinen, C.D. (2022). A calibrated cell-based functional assay to aide classification of MLH1 DNA mismatch repair gene variants. Hum. Mutat. https://doi.org/10.1002/humu.24462.

Sato, T., Stange, D.E., Ferrante, M., Vries, R.G.J., van Es, J.H., van den Brink, S., van Houdt, W.J., Pronk, A., van Gorp, J., Siersema, P.D., and Clevers, H. (2011). Long-term expansion of epithelial organoids from human colon, adenoma, adenocarcinoma, and Barrett's epithelium. Gastroenterology *141*, 1762–1772.

Sato, T., Vries, R.G., Snippert, H.J., van de Wetering, M., Barker, N., Stange, D.E., van Es, J.H., Abo, A., Kujala, P., Peters, P.J., and Clevers, H. (2009). Single Lgr5 stem cells build crypt–villus structures in vitro without a mesenchymal niche. Nature *459*, 262–265.

Staffa, L., Echterdiek, F., Nelius, N., Benner, A., Werft, W., Lahrmann, B., Grabe, N., Schneider, M., Tariverdian, M., von Knebel Doeberitz, M., et al. (2015). Mismatch repair-deficient crypt foci in Lynch syndrome – molecular alterations and association with clinical parameters. PLoS One *10*, e0121980.

Strand, M., Prolla, T.A., Liskay, R.M., and Petes, T.D. (1993). Destabilization of tracts of simple repetitive DNA in yeast by mutations affecting DNA mismatch repair. Nature *365*, 274–276.

Suzuki, H., Harpaz, N., Tarmin, L., Yin, J., Jiang, H.-Y., Bell, J.D., Hontanosas, M., Groisman, G.M., Abraham, J.M., and Meltzer, S.J. (1994). Microsatellite instability in ulcerative colitis-associated colorectal dysplasias and cancers. Cancer Res. *54*, 4841–4844.

Swann, P.F., Waters, T.R., Moulton, D.C., Xu, Y.Z., Zheng, Q., Edwards, M., and Mace, R. (1996). Role of postreplicative DNA mismatch repair in the cytotoxic action of thioguanine. Science *273*, 1109–1111.

Tahara, T., Inoue, N., Hisamatsu, T., Kashiwagi, K., Takaishi, H., Kanai, T., Watanabe, M., Ishii, H., and Hibi, T. (2005). Clinical significance of microsatellite instability in the inflamed mucosa for the prediction of colonic neoplasms in patients with ulcerative colitis. J. Gastroenterol. Hepatol. *20*, 710–715.

Todoric, J., Antonucci, L., and Karin, M. (2016). Targeting inflammation in cancer prevention and therapy. Cancer Prev. Res. *9*, 895–905.

Walsh, M.D., Buchanan, D.D., Pearson, S.-A., Clendenning, M., Jenkins, M.A., Win, A.K., Walters, R.J., Spring, K.J., Nagler, B., Pavluk, E., et al. (2012). Immunohistochemical testing of conventional adenomas for loss of expression of mismatch repair proteins in Lynch syndrome mutation carriers: a case series from the Australasian site of the colon cancer family registry. Mod. Pathol. *25*, 722–730.

Wang, G., Alamuri, P., Humayun, M.Z., Taylor, D.E., and Maier, R.J. (2005). The Helicobacter pylori MutS protein confers protection from oxidative DNA damage. Mol. Microbiol. *58*, 166–176.

Wang, X., Lin, G., Martins-Taylor, K., Zeng, H., and Xu, R.H. (2009). Inhibition of caspase-mediated anoikis is critical for basic fibroblast growth factor-sustained culture of human pluripotent stem cells. J. Biol. Chem. *284*, 34054–34064.

Watanabe, K., Ueno, M., Kamiya, D., Nishiyama, A., Matsumura, M., Wataya, T., Takahashi, J.B., Nishikawa, S.i., Nishikawa, S., Muguruma, K., and Sasai, Y. (2007). A ROCK inhibitor permits survival of dissociated human embryonic stem cells. Nat. Biotechnol. *25*, 681–686.

Watson, P., Ashwathnarayan, R., Lynch, H.T., and Roy, H.K. (2004). Tobacco use and increased colorectal cancer risk in patients with hereditary nonpolyposis colorectal cancer (Lynch syndrome). Arch. Intern. Med. *164*, 2429–2431.

Winkels, R.M., Botma, A., Van Duijnhoven, F.J.B., Nagengast, F.M., Kleibeuker, J.H., Vasen, H.F.A., and Kampman, E. (2012). Smoking increases the risk for colorectal adenomas in patients with Lynch syndrome. Gastroenterology *142*, 241–247.

Wojciechowicz, K., Cantelli, E., Van Gerwen, B., Plug, M., Van Der Wal, A., Delzenne-Goette, E., Song, J.-Y., De Vries, S., Dekker, M., and Te Riele, H. (2014). Temozolomide increases the number of mismatch repair–deficient intestinal crypts and accelerates tumorigenesis in a mouse model of Lynch syndrome. Gastroenterology *147*, 1064–1072.e5.

Yang, G., Scherer, S.J., Shell, S.S., Yang, K., Kim, M., Lipkin, M., Kucherlapati, R., Kolodner, R.D., and Edelmann, W. (2004). Dominant effects of an Msh6 missense mutation on DNA repair and cancer susceptibility. Cancer Cell *6*, 139–150.

Yip, H.Y.K., Tan, C.W., Hirokawa, Y., and Burgess, A.W. (2018). Colon organoid formation and cryptogenesis are stimulated by growth factors secreted from myofibroblasts. PLoS One *13*, e0199412.

Yurgelun, M.B., Goel, A., Hornick, J.L., Sen, A., Turgeon, D.K., Ruffin, M.T., Marcon, N.E., Baron, J.A., Bresalier, R.S., Syngal, S., et al. (2012). Microsatellite instability and DNA mismatch repair protein deficiency in Lynch syndrome colorectal polyps. Cancer Prev. Res. *5*, 574–582.

Zeng, H., Guo, M., Martins-Taylor, K., Wang, X., Zhang, Z., Park, J.W., Zhan, S., Kronenberg, M.S., Lichtler, A., Liu, H.-X., et al. (2010). Specification of region-specific neurons including forebrain glutamatergic neurons from human induced pluripotent stem cells. PLoS One *5*, e11853.